Acta Cryst E
CRYSTALLOGRAPHIC COMMUNICATIONS
ISSN 2056-9890

Synthesis, crystal structure and Hirshfeld surface analysis of 5,5-diphenyl-3-(prop-2-yn-1-yl)-imidazolidine-2,4-dione

Abderrazzak El Moutaouakil Ala Allah,[a] Chiara Massera,[b] Walid Guerrab,[a] Abdulsalam Alsubari,[c]* Joel T. Mague[d] and Youssef Ramli[a]*

[a]Laboratory of Medicinal Chemistry, Drug Sciences Research Center, Faculty of Medicine and Pharmacy, Mohammed V University in Rabat, Morocco, [b]Dipartimento di Scienze Chimiche, della Vita e della Sostenibilità Ambientale, Università di Parma, Parco Area delle Scienze 17/A 43124 Parma, Italy, [c]Laboratory of Medicinal Chemistry, Faculty of Clinical Pharmacy, 21 September University, Yemen, and [d]Department of Chemistry, Tulane University, New Orleans, LA 70118, USA. *Correspondence e-mail: alsubaripharmaco@21umas.edu.ye, y.ramli@um5r.ac.ma

Received 17 March 2025
Accepted 15 April 2025

Edited by L. Van Meervelt, Katholieke Universiteit Leuven, Belgium

Keywords: crystal structure; hydantoin; alkylation; Hirshfeld surface analysis.

CCDC reference: 2444171

Supporting information: this article has supporting information at journals.iucr.org/e

The new phenytoin analogue 5,5-diphenyl-3-(2-propyn-1-yl)imidazolidine-2,4-dione, $C_{18}H_{14}N_2O_2$ (**3**), was obtained through an alkylation reaction with propargyl bromide *via* the phase-transfer catalysis method, and its structure was determined *via* single-crystal X-ray diffraction analysis. The asymmetric unit of **3** consists of two independent molecules differing mainly in the orientation of the propynyl group. Each molecule forms an inversion dimer through pairs of N2—H2···O2 hydrogen bonds. The crystal structure is further consolidated by C—H···O and C—H···π interactions. The contributions of the different interactions towards the crystal packing were further analysed using Hirshfeld surface and fingerprint plots, showing that the largest contribution comes from the H···H contacts (45%).

1. Chemical context

Hydantoin, also known as glycolylurea or 2,4-imidazolidinedione, is a saturated heterocyclic compound derived from imidazole. Phenytoin, 5,5-diphenylimidazolidine-2,4-dione, is a molecule belonging to the hydantoin group, which is used in pharmacy mainly as an antiepileptic (Giunchi *et al.*, 2019; El Moutaouakil Ala Allah *et al.*, 2024*a*). The main site of action appears to be the motor cortex, where it inhibits the spread of seizure activity. Phenytoin is indicated for the control of grand mal and psychomotor seizures (Guerrab *et al.*, 2022*a*). It is also applicable for various diseases, as it has antiarrhythmic (Handzlik *et al.*, 2012), anti-HIV (Vamecq *et al.*, 1998), cytotoxic (Guerrab *et al.*, 2023*a*), antiproliferative (Aboeldahab *et al.*, 2018) and antibacterial effects (El Moutaouakil Ala Allah *et al.*, 2024*b*). Various methods for synthesizing hydantoins have been reported, including the reaction of benzyls with urea in an ethanolic solution of potassium or sodium hydroxide (Guerrab *et al.*, 2022*b*, 2023*b*; Allah *et al.*, 2024; El Moutaouakil Ala Allah *et al.*, 2023). Moreover, alkylation-based chemical modifications of phenytoin are seen to strengthen and expand its biological activity (Guerrab *et al.*, 2020*a*). Some analogs have also been synthesized and evaluated for their industrial properties (*e.g.* Ettahiri *et al.*, 2024). Our interest in hydantoins results from their simple synthesis and the ease with which X-ray quality crystals can be grown. In this context, we present in this study a new phenytoin obtained through an alkylation reaction with propargyl bromide *via* the phase-transfer catalysis method. This paper presents the crystal structure of novel phenytoin analogue **3**. A

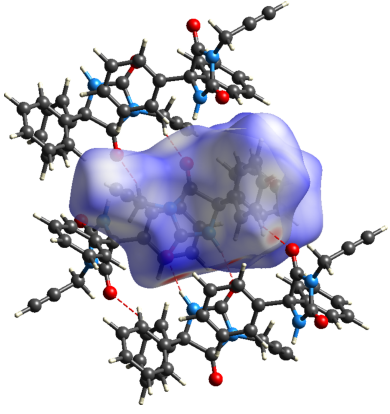

Hirshfeld surface analysis was performed to analyze the intermolecular interactions.

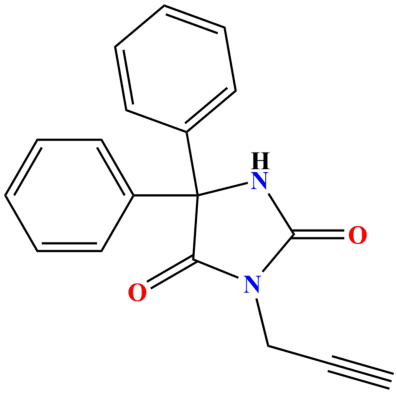

2. Structural commentary

The asymmetric unit consists of two independent molecules (*A* and *B*) differing modestly in the rotational orientations of the phenyl rings and most obviously in the orientation of the propynyl group (Fig. 1). Thus the C2*A*—N1*A*—C4*A*—C41*A* torsion angle is −80.1 (2)°, while C2*B*—N1*B*—C4*B*—C41*B* is −68.4 (2)°. The overlay of molecule *A* (red) and molecule *B* (blue) is shown in Fig. 2; the r.m.s. deviation for non-H atoms is 0.325 Å. As in many related molecules, the dihedral angles between the mean planes of the five-membered ring and those of the phenyl rings is larger than 50°. In molecule *A*, these are 53.58 (8) and 56.68 (9)° while in molecule *B*, they are 56.81 (8) and 74.26 (9)°, another indication of the different conformations of the two independent molecules. Bond lengths and interbond angles are as expected for this type of compound. The five-membered rings C1*A*–C3*A*/N1*A*/N2*A* (ring *A*) and C1*B*–C3*B*/N1*B*/N2*B* (ring *B*) are both essentially planar, with r.m.s. deviations of 0.010 and 0.044 and Å, respectively. For ring *A*, atom N1*A* shows the largest deviation [0.009 (1) Å], while atoms O1*A* and O2*A* deviate by −0.035 (1) and 0.028 (1) Å from the mean plane. For ring *B*, the largest deviation of −0.038 (2) Å is shown by atom C2*B*, while atoms O1*B* and O2*B* deviate −0.097 (1) and −0.047 (1) Å from the mean plane.

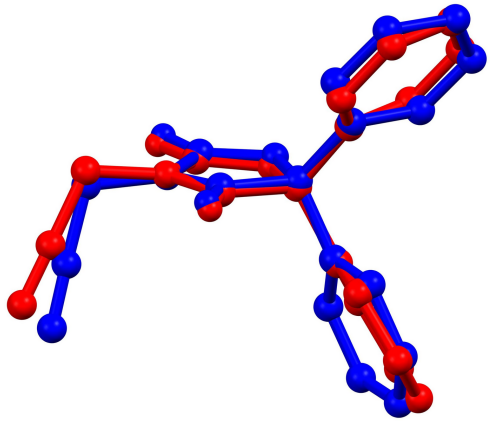

Figure 2
Overlay of molecules *A* (red) and *B* (blue) present in the asymmetric unit of the title compound.

3. Supramolecular features

In the crystal, each independent molecule forms an inversion dimer through pairs of N2—H2···O2 (*A* or *B*) hydrogen bonds (Table 1). For molecule *A*, these dimers are connected into chains extending along the *b*-axis direction by inversion-related C4*A*—H4*AA*···O1*A* hydrogen bonds (Table 1 and Fig. 3). The dimers of molecule *B* are linked to the above-mentioned chains by C15*A*—H15*A*···O1*B* hydrogen bonds and C8*B*—H8*B*···*Cg*2 interactions (Table 1 and Fig. 3). These supramolecular aggregates are in turn connected by C15*B*—H15*B*···*Cg*3 interactions (Table 1). *Cg*2 and *Cg*3 are the centroids of the C5*A*–C10*A* and C11*A*–C16*A* benzene rings, respectively.

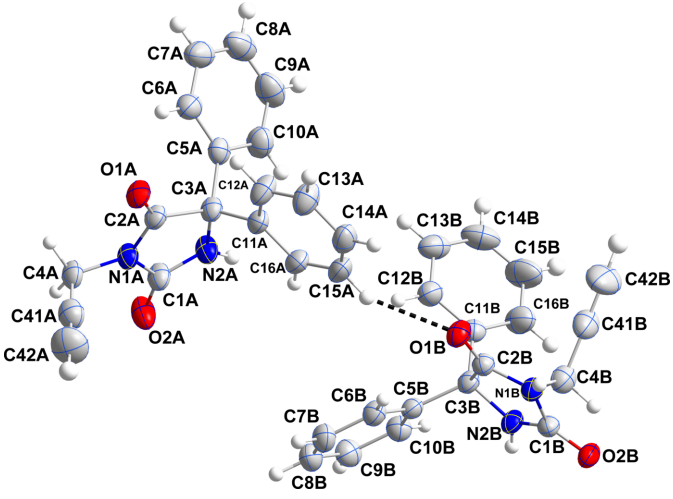

Figure 1
The asymmetric unit with labeling scheme and 50% probability ellipsoids. The C—H···O hydrogen bond is depicted by a dashed line.

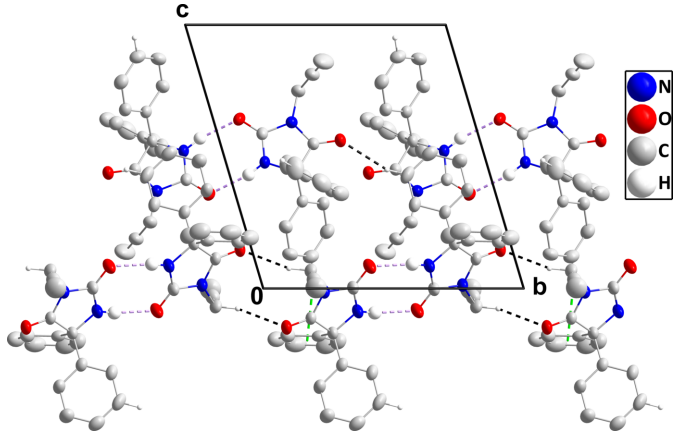

Figure 3
Packing viewed along the *a*-axis direction with N—H···O and C—H···O hydrogen bonds depicted, respectively, by violet and black dashed lines. The C—H···π(ring) interactions are depicted by green dashed lines and non-interacting hydrogen atoms are omitted for clarity.

Table 1
Hydrogen-bond geometry (Å, °).

*Cg*2 and *Cg*3 are the centroids of the C5*A*–C10*A* and C11*A*–C16*A* benzene rings, respectively.

D—H···*A*	*D*—H	H···*A*	*D*···*A*	*D*—H···*A*
N2*A*—H2*A*···O2*A*^{i}	0.88 (2)	1.99 (2)	2.855 (2)	167 (2)
N2*B*—H2B*B*···O2*B*^{ii}	0.89 (2)	1.99 (2)	2.847 (1)	163 (2)
C4*A*—H4*AA*···O1*A*^{iii}	0.99	2.31	3.253 (2)	160
C15*A*—H15*A*···O1*B*	0.95	2.44	3.332 (2)	156
C8*B*—H8*B*···*Cg*2^{i}	0.95	2.88	3.713 (2)	147
C15*B*—H15*B*···*Cg*3^{iv}	0.95	2.87	3.742 (3)	153

Symmetry codes: (i) $-x+1, -y+1, -z$; (ii) $-x+1, -y, -z+1$; (iii) $-x+1, -y+2, -z$; (iv) $-x+2, -y+1, -z+1$.

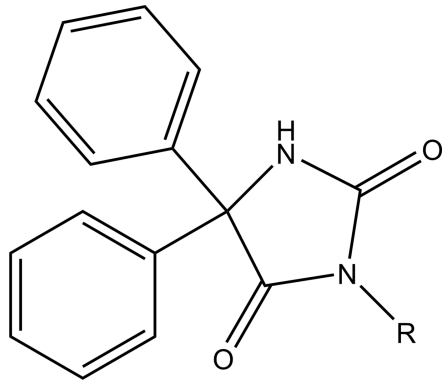

Figure 4
The search fragment used for the database search.

4. Database survey

A search of the Cambridge Structural Database (CSD, 2023.3.1; Groom *et al.*, 2016) with the fragment shown in Fig. 4 (*R* = C) yielded 25 structures, of which 19 were deemed closest to the title molecule, since all of the substituents, *R*, were mainly hydrocarbon groups. These are listed in Table 2 from which it is apparent that the dihedral angles between the mean planes of the two phenyl groups and that of the five-membered ring to which they are attached range from 51.23 (6)° (WUGCEJ) to as large as 83.89 (16)° (YOFMUE). The two angles may also be nearly equal as in FEHPUG or differ by as much as 31.81° as in WUGCEJ. The range of dihedral angles and the difference between them in a particular molecule is likely due to packing considerations, but there does not appear to be a simple correlation with the space group or the size of the substituent *R*.

5. Hirshfeld surface analysis

CrystalExplorer (Spackman *et al.*, 2021) was used to perform the Hirshfeld surface (HS) analysis. A full description of the procedures and the interpretation of the results obtained has been published (Tan *et al.*, 2019). Fig. 5 presents the d_{norm} surface for molecule *A*, together with several near neighbors consisting of both molecules *A* and *B*. A portion of the chain of dimers formed by the *A* molecules can be seen in the center of the figure, while at the bottom of the surface the N—H···O hydrogen bonds are shown as two intense red spots. The lighter red spot at the lower right corresponds to the C—H···O hydrogen bond that links molecules *A* and *B*. Fig. 6 shows the 2-D fingerprint plots for all intermolecular interactions (*a*) and those specifically representing H···H (*b*), C···H/H···C (*c*) and O···H/H···O (*d*) interactions. The largest contribution to the intermolecular interactions comes from the H···H contacts (45%), which is consistent with the periphery of the molecule being largely hydrogen in nature and can be attributed to van der Waals contacts. The C···H/H···C contacts contribute 32.1% and appear as a pair of blunt peaks at $d_e + d_i \simeq 3.2$ Å. These can be primarily attributed to the C—H···π(ring) interactions. The last significant contribution is from the O···H/H···O interactions (17.9%) which appear as a pair of sharp spikes at $d_e + d_i \simeq 2.2$ Å. These represent the N—H···O and the C—H···O hydrogen bonds, respectively. All other intermolecular contacts, *e.g.* N···H/H···N, C···N, O···C, *etc.*, contribute less than 2% to the total. The HS surface for molecule *B* is virtually identical to that for

Table 2
Dihedral angles (°) between the phenyl rings and the five-membered ring for related molecules.

R	Refcode	Dihedral angles	Reference
Me	PEPDUM	59.17 (6), 53.21 (6)	Guerrab *et al.* (2017*a*)
Et	FEHPUG	64.03 (5), 63.04 (5)	Guerrab *et al.* (2017*b*)
2-bromoethyl	NIBMOE	63.60 (16), 76.45 (16)	Guerrab *et al.* (2023*a*)
allyl	BUCDEL	62.07 (13), 64.55 (12)	Guerrab *et al.* (2020*a*)
n-propyl	WEMQUD	66.09 (8), 67.12 (8); 64.48 (8), 71.25 (8)	Guerrab *et al.* (2017*c*)
n-propyl	WEMQUD01	64.6 (8), 69.3 (8)	Trišović *et al.* (2019)
i-propyl	YOFMOY	56.86 (11), 79.79 (11)	Trišović *et al.* (2019)
cyclopropyl	YOFMUE	59.52 (15), 83.89 (16)	Trišović *et al.*, 2019)
i-butyl	QENBET	50.08 (6), 66.31 (5)	Guerrab *et al.* (2018*a*)
s-butyl	YEDYOZ	68.42 (5), 73.04 (5)	Guerrab *et al.* (2022*b*)
t-butyl	YOFNAL	66.8 (2), 73.8 (2)	Trišović *et al.* (2019)
n-pentyl	YOFNEP	63.41 (16), 75.12 (16)	Trišović *et al.* (2019)
n-hexyl	GEMSOJ	63.6 (8), 70.4 (8)	Guerrab *et al.* (2017*d*)
n-octyl	QENBOD	69.71 (12), 71.80 (12); 71.24 (11), 67.85 (12)	Guerrab *et al.* (2018*b*)
n-nonyl	QAGPAT	76.0 (8), 63.5 (8)	Guerrab *et al.* (2020*b*)
n-decyl	PAJMAS	54.03 (7), 60.67 (7)	Guerrab *et al.* (2021)
benzyl	MESSAH	71.65 (6), 71.62 (6); 76.38 (6), 70.22 (6)	Guerrab *et al.* (2018*c*)
phenyl	WUGCEJ	51.23 (6), 83.04 (6)	Berntsen *et al.* (2020)
m-tolyl	WUGCIN	67.28 (8), 65.51 (8)	Berntsen *et al.* (2020)

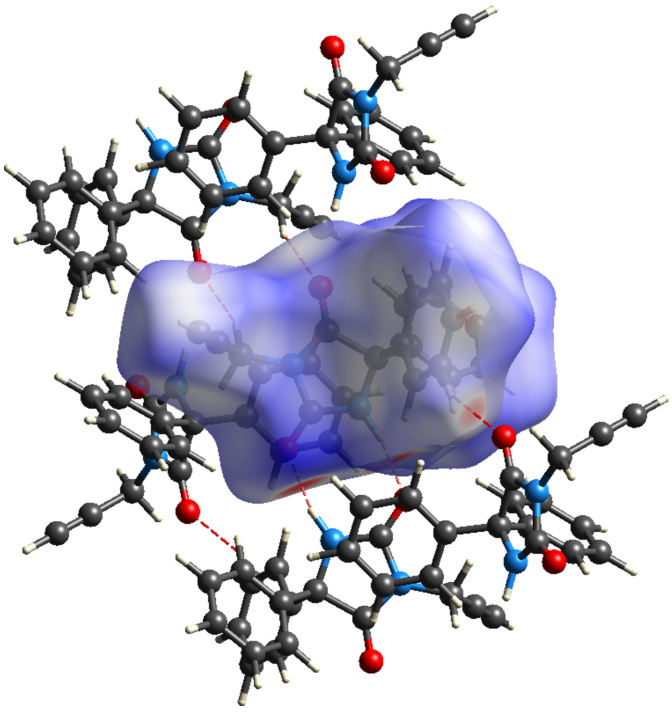

Figure 5
The d_{norm} surface for molecule *A* with nearest neighbor molecules *A* and *B*. The intermolecular hydrogen bonds are depicted by red dashed lines.

molecule *A* as are the 2-D fingerprint plots. The only difference is in the percentage contribution to the overall intermolecular interactions. For molecule *B* these are 40.3% for

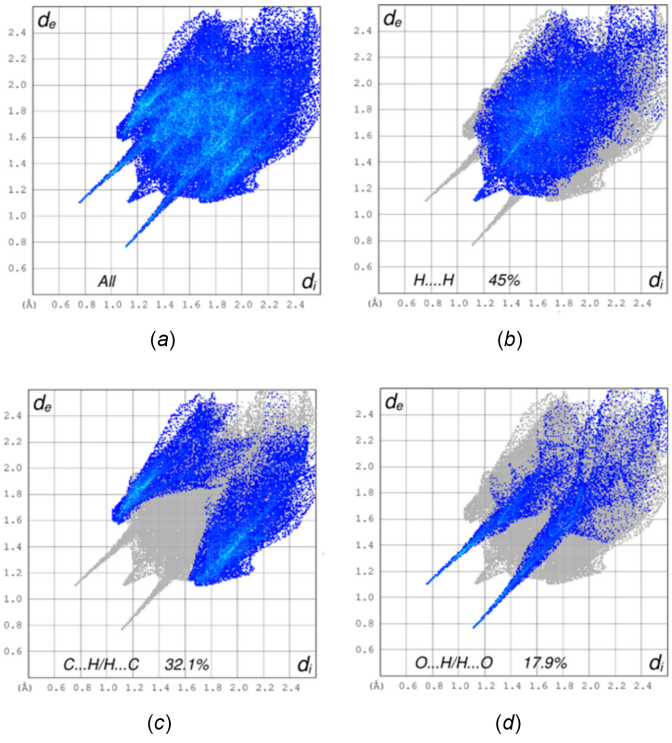

Figure 6
Two-dimensional fingerprint plots showing all intermolecular interactions (*a*) and those showing just H···H contacts (*b*), C···H/H···C contacts (*c*) and O···H/H···O contacts (*d*).

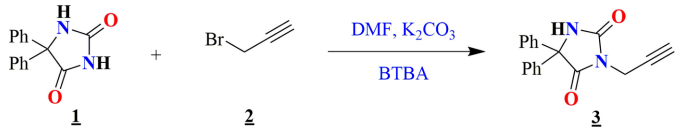

Figure 7
Reaction scheme for the formation of the title compound **3**.

H···H contacts, 34.7% for C···H/H···C contacts and 18.8% for O···H/H···O contacts. Again, other contacts are less than 2% each.

6. Synthesis and crystallization

The reaction scheme for the synthesis of the title compound is shown in Fig. 7. To a solution of phenytoin **1** (0.5 g, 2 mmol) in DMF (10 mL), in the presence of K_2CO_3 (2.2 mmol), propargyl bromide **2** (2.2 mmol) was added dropwise along with a catalytic amount of BTBA (benzyl tributyl ammonium bromide). The mixture was stirred at room temperature for 2 h. After filtration of the salts, the solvent was evaporated, and the resulting residue was purified by recrystallization in ethanol, yielding colorless crystals of **3**.

Yield = 96%, **m.p.** = 408–410 K. **FT-IR** (ATR, cm^{-1}): 3375 (CH propargyl), 3060–3080, (CH aromatic), 1765 (C═O); **^{1}H NMR** (500 MHz, DMSO-d_6): δ ppm 3.22 (*t*, 1H, CH propargyl), 4,22 (*s*, 2H, N—CH_2), 7.03–7.42 (*m*, 10, Ar—H), 9.78 (*s*, 1H, NH); **^{13}C NMR**: 28.01 (N—CH_2); 74.40 (CH propargyl); 69.71 (C—2Ph); 74.40 (C_q propargyl); 127.25, 128.00, 128.58, 140.15 (C—Ar); 154.57 (C═O); 172.73 (C═O). **HRMS (ESI)**: calculated for $C_{18}H_{14}N_2O_2$ $[M + H]^+$ 291.1055; found 291.1122.

7. Refinement

Crystal data, data collection and structure refinement details are summarized in Table 3. The carbon-bound H atoms were placed in calculated positions and refined isotropically using the riding model, with C—H distances ranging from 0.95 to 0.99 Å and U_{iso}(H) set to 1.2–1.5U_{eq}(C). The H atoms H2*A* and H2*B* of the two imidazole rings were found in a difference-Fourier map and refined freely.

Acknowledgements

CM would like to acknowledge the COMP-*R* Initiatives, funded by the "Departments of Excellence" program of the Italian Ministry for University and Research (MUR, 2023–2027). YR is thankful to the National Center for Scientific and Technical Research of Morocco (CNRST) for its continuous support. The contributions of the authors are as follows: conceptualization, YR; methodology, AA; investigation, AEMAA and WG; writing (original draft), AEMAA; writing (review and editing of the manuscript), YR; formal analysis, JTM and CM; supervision, YR; crystal structure determination, CM.

References

Aboeldahab, A. M. A., Beshr, E. A. M., Shoman, M. E., Rabea, S. M. & Aly, O. M. (2018). *Eur. J. Med. Chem.* **146**, 79–92.

Akrad, R., Guerrab, W., Lazrak, F., Ansar, M., Taoufik, J., Mague, J. T. & Ramli, Y. (2018*c*). *IUCrData*, **3**, x180934.

Allah, A. E. M. A., Temel, E., Guerrab, W., Nchioua, I., Mague, J. T., Talbaoui, A., Alzahrani, A. Y. A. & Ramli, Y. (2024). *J. Mol. Struct.* **1312**, 138572.

Allen, F. H., Johnson, O., Shields, G. P., Smith, B. R. & Towler, M. (2004). *J. Appl. Cryst.* **37**, 335–338.

Brandenburg, K. & Putz, H. (2012). *DIAMOND*. Crystal Impact GbR, Bonn, Germany.

Bruker (2016). *APEX3* and *SAINT*. Bruker AXS, Madison, Wisconsin, USA.

El Moutaouakil Ala Allah, A., Guerrab, W., Alsubari, A., Mague, J. T. & Ramli, Y. (2023). *IUCrData*, **8**, x230208.

El Moutaouakil Ala Allah, A., Guerrab, W., Maatallah, M., Mague, J. T., Talbaoui, A., Alzahrani, A. Y. A. & Ramli, Y. (2024*a*). *J. Mol. Struct.* **1310**, 138324.

El Moutaouakil Ala Allah, A., Said, M. A., Al-Kaff, N. S., Mague, J. T., Demirtaş, G. & Ramli, Y. (2024*b*). *J. Mol. Struct.* **1318**, 139430.

Ettahiri, W., El Moutaouakil Ala Allah, A., Lazrak, J., Safir, E. H., Yadav, K. K., Hammouti, B., Obaidullah, A. J., Rais, Z., Ramli, Y. & Taleb, M. (2024). *J. Ind. Eng. Chem.* **140**, 631–646.

Farrugia, L. J. (2012). *J. Appl. Cryst.* **45**, 849–854.

Giunchi, A., Rivalta, A., Bedoya-Martínez, N., Schrode, B., Braun, D. E., Werzer, O., Venuti, E. & Della Valle, R. G. (2019). *Cryst. Growth Des.* **19**, 6067–6073.

Groom, C. R., Bruno, I. J., Lightfoot, M. P. & Ward, S. C. (2016). *Acta Cryst.* B**72**, 171–179.

Guerrab, W., Akachar, J., Jemli, M. E., Abudunia, A.-M., Ouaabou, R., Alaoui, K., Ibrahimi, A. & Ramli, Y. (2023*b*). *J. Biomol. Struct. Dyn.* **41**, 4592–4600.

Guerrab, W., Akrad, R., Ansar, M., Taoufik, J., Mague, J. T. & Ramli, Y. (2017*a*). *IUCrData*, **2**, x171534.

Guerrab, W., Akrad, R., Ansar, M., Taoufik, J., Mague, J. T. & Ramli, Y. (2017*b*). *IUCrData*, **2**, x171591.

Guerrab, W., Akrad, R., Ansar, M., Taoufik, J., Mague, J. T. & Ramli, Y. (2017*d*). *IUCrData*, **2**, x171693.

Guerrab, W., El Jemli, M., Akachar, J., Demirtas, G., Mague, J. T., Taoufik, J., Ibrahimi, A., Ansar, M., Alaoui, K. & Ramli, Y. (2021). *J. Biomol. Struct. Dyn.* **40**, 8765–8782.

Guerrab, W., El Jemli, M., Akachar, J., Demirtaş, G., Mague, J. T., Taoufik, J., Ibrahimi, A., Ansar, M., Alaoui, K. & Ramli, Y. (2022*a*). *J. Biomol. Struct. Dyn.* **40**, 8765–8782.

Guerrab, W., El Moutaouakil Ala Allah, A., Alsubari, A., Mague, J. T. & Ramli, Y. (2022*b*). *IUCrData*, **7**, x220598.

Guerrab, W., El Moutaouakil Ala Allah, A., Alsubari, A., Mague, J. T. & Ramli, Y. (2023*a*). *IUCrData*, **8**, x230060.

Guerrab, W., Lgaz, H., Kansiz, S., Mague, J. T., Dege, N., Ansar, M., Marzouki, R., Taoufik, J., Ali, I. H., Chung, I. & Ramli, Y. (2020*a*). *J. Mol. Struct.* **1205**, 127630.

Guerrab, W., Mague, J. T., Akrad, R., Ansar, M., Taoufik, J. & Ramli, Y. (2017*c*). *IUCrData*, **2**, x171808.

Guerrab, W., Mague, J. T. & Ramli, Y. (2020*b*). *Z. Kristallogr. New Cryst. Struct.* **235**, 1425–1427.

Guerrab, W., Mague, J. T., Taoufik, J. & Ramli, Y. (2018*b*). *IUCrData*, **3**, x180057.

Guerrab, W., Mague, J. T., Akrad, R., Ansar, M., Taoufik, J. & Ramli, Y. (2018*a*). *IUCrData*, **3**, x180050.

Table 3
Experimental details.

Crystal data	
Chemical formula	$C_{18}H_{14}N_2O_2$
M_r	290.31
Crystal system, space group	Triclinic, $P\overline{1}$
Temperature (K)	200
a, b, c (Å)	11.3526 (3), 12.0162 (3), 13.3087 (3)
α, β, γ (°)	97.080 (1), 114.406 (1), 107.335 (1)
V (Å^3)	1513.47 (7)
Z	4
Radiation type	Cu $K\alpha$
μ (mm^{-1})	0.68
Crystal size (mm)	0.17 × 0.15 × 0.10
Data collection	
Diffractometer	Bruker D8 Venture PhotonII
Absorption correction	Multi-scan (*SADABS*; Krause et al., 2015)
T_{min}, T_{max}	0.639, 0.754
No. of measured, independent and observed [$I > 2\sigma(I)$] reflections	17923, 5879, 5126
R_{int}	0.040
$(\sin \theta/\lambda)_{max}$ (Å^{-1})	0.618
Refinement	
$R[F^2 > 2\sigma(F^2)]$, $wR(F^2)$, S	0.040, 0.117, 1.02
No. of reflections	5879
No. of parameters	406
H-atom treatment	H atoms treated by a mixture of independent and constrained refinement
$\Delta\rho_{max}$, $\Delta\rho_{min}$ (e Å^{-3})	0.23, −0.23

Computer programs: *APEX3* and *SAINT* (Bruker, 2016), *SHELXT2018/2* (Sheldrick, 2015*a*), *SHELXL2019/2* (Sheldrick, 2015*b*), *Mercury* (Macrae *et al.*, 2020) *DIAMOND* (Brandenburg & Putz, 2012), *WinGX* (Farrugia, 2012), *publCIF* (Westrip, 2010) and *enCIFer* (Allen *et al.*, 2004).

Handzlik, J., Bajda, M., Zygmunt, M., Maciąg, D., Dybała, M., Bednarski, M., Filipek, B., Malawska, B. & Kieć-Kononowicz, K. (2012). *Bioorg. Med. Chem.* **20**, 2290–2303.

Krause, L., Herbst-Irmer, R., Sheldrick, G. M. & Stalke, D. (2015). *J. Appl. Cryst.* **48**, 3–10.

Macrae, C. F., Sovago, I., Cottrell, S. J., Galek, P. T. A., McCabe, P., Pidcock, E., Platings, M., Shields, G. P., Stevens, J. S., Towler, M. & Wood, P. A. (2020). *J. Appl. Cryst.* **53**, 226–235.

Neerbye Berntsen, L., Nova, A., Wragg, D. S. & Sandtorv, A. H. (2020). *Org. Lett.* **22**, 2687–2691.

Sheldrick, G. M. (2015*a*). *Acta Cryst.* A**71**, 3–8.

Sheldrick, G. M. (2015*b*). *Acta Cryst.* C**71**, 3–8.

Spackman, P. R., Turner, M. J., McKinnon, J. J., Wolff, S. K., Grimwood, D. J., Jayatilaka, D. & Spackman, M. A. (2021). *J. Appl. Cryst.* **54**, 1006–1011.

Tan, S. L., Jotani, M. M. & Tiekink, E. R. T. (2019). *Acta Cryst.* E**75**, 308–318.

Trišović, N., Radovanović, L., Janjić, G. V., Jelić, S. T. & Rogan, J. (2019). *Cryst. Growth Des.* **19**, 2163–2174.

Vamecq, J., Van derpoorten, K., Poupaert, J. H., Balzarini, J., De Clercq, E. & Stables, J. P. (1998). *Life Sci.* **63**, L267–P, L274.

Westrip, S. P. (2010). *J. Appl. Cryst.* **43**, 920–925.

supporting information

Acta Cryst. (2025). E**81**, 412-416 [https://doi.org/10.1107/S2056989025003391]

Synthesis, crystal structure and Hirshfeld surface analysis of 5,5-diphenyl-3-(prop-2-yn-1-yl)imidazolidine-2,4-dione

Abderrazzak El Moutaouakil Ala Allah, Chiara Massera, Walid Guerrab, Abdulsalam Alsubari, Joel T. Mague and Youssef Ramli

Computing details

5,5-Diphenyl-3-(2-propyn-1-yl)imidazolidine-2,4-dione

Crystal data

$C_{18}H_{14}N_2O_2$
M_r = 290.31
Triclinic, $P\overline{1}$
a = 11.3526 (3) Å
b = 12.0162 (3) Å
c = 13.3087 (3) Å
α = 97.080 (1)°
β = 114.406 (1)°
γ = 107.335 (1)°
V = 1513.47 (7) Å^3
Z = 4
F(000) = 608
D_x = 1.274 Mg m^{-3}
Cu $K\alpha$ radiation, λ = 1.54178 Å
Cell parameters from 1278 reflections
θ = 3.8–72.3°
μ = 0.68 mm^{-1}
T = 200 K
Prismatic, colourless
0.17 × 0.15 × 0.10 mm

Data collection

Bruker D8 Venture PhotonII diffractometer
Radiation source: fine-focus sealed tube
Graphite monochromator
phi & ω scan
Absorption correction: multi-scan (SADABS; Krause et al., 2015)
T_{min} = 0.639, T_{max} = 0.754
17923 measured reflections
5879 independent reflections
5126 reflections with $I > 2\sigma(I)$
R_{int} = 0.040
θ_{max} = 72.3°, θ_{min} = 3.8°
h = −13→13
k = −14→14
l = −16→16

Refinement

Refinement on F^2
Least-squares matrix: full
$R[F^2 > 2\sigma(F^2)]$ = 0.040
$wR(F^2)$ = 0.117
S = 1.02
5879 reflections
406 parameters
0 restraints
Hydrogen site location: mixed
H atoms treated by a mixture of independent and constrained refinement
$w = 1/[\sigma^2(F_o^2) + (0.0647P)^2 + 0.2418P]$ where $P = (F_o^2 + 2F_c^2)/3$
$(\Delta/\sigma)_{max}$ < 0.001
$\Delta\rho_{max}$ = 0.23 e Å^{-3}
$\Delta\rho_{min}$ = −0.23 e Å^{-3}
Extinction correction: SHELXL-2019/2 (Sheldrick 2015*b*), $Fc^*=kFc[1+0.001xFc^2\lambda^3/\sin(2\theta)]^{-1/4}$
Extinction coefficient: 0.0056 (5)

Special details

Geometry. All esds (except the esd in the dihedral angle between two l.s. planes) are estimated using the full covariance matrix. The cell esds are taken into account individually in the estimation of esds in distances, angles and torsion angles; correlations between esds in cell parameters are only used when they are defined by crystal symmetry. An approximate (isotropic) treatment of cell esds is used for estimating esds involving l.s. planes.

Fractional atomic coordinates and isotropic or equivalent isotropic displacement parameters (Å²)

	x	*y*	*z*	U_{iso}*/U_{eq}
O1A	0.59193 (10)	0.95473 (8)	0.14741 (8)	0.0443 (2)
O2A	0.38335 (12)	0.56618 (9)	−0.08410 (9)	0.0588 (3)
N1A	0.46487 (12)	0.76899 (9)	0.01292 (9)	0.0390 (2)
N2A	0.59068 (12)	0.66309 (10)	0.08644 (10)	0.0436 (3)
C1A	0.47235 (15)	0.65472 (11)	−0.00263 (12)	0.0426 (3)
C2A	0.57528 (13)	0.85052 (10)	0.11236 (11)	0.0361 (3)
C3A	0.67094 (13)	0.78384 (10)	0.16927 (10)	0.0360 (3)
C4A	0.35230 (15)	0.79744 (12)	−0.06815 (11)	0.0424 (3)
H4AA	0.392791	0.878766	−0.076517	0.051*
H4AB	0.306232	0.737385	−0.144406	0.051*
C41A	0.24764 (17)	0.79629 (13)	−0.03154 (13)	0.0513 (4)
C42A	0.1633 (2)	0.7962 (2)	−0.0025 (2)	0.0825 (6)
H42A	0.094924	0.796197	0.021040	0.099*
C5A	0.81762 (14)	0.84068 (12)	0.18064 (10)	0.0391 (3)
C6A	0.87396 (15)	0.95894 (13)	0.17795 (12)	0.0481 (3)
H6A	0.819765	1.007611	0.166135	0.058*
C7A	1.00935 (18)	1.00670 (17)	0.19244 (15)	0.0630 (4)
H7A	1.046191	1.087114	0.188360	0.076*
C8A	1.09019 (18)	0.9387 (2)	0.21258 (15)	0.0672 (5)
H8A	1.183203	0.972144	0.223631	0.081*
C9A	1.03585 (19)	0.8221 (2)	0.21666 (16)	0.0667 (5)
H9A	1.091751	0.774849	0.230654	0.080*
C10A	0.90012 (17)	0.77223 (16)	0.20059 (14)	0.0543 (4)
H10A	0.863499	0.691147	0.203234	0.065*
C11A	0.68600 (13)	0.78422 (11)	0.28908 (11)	0.0366 (3)
C12A	0.74629 (18)	0.89481 (13)	0.37237 (12)	0.0505 (3)
H12A	0.773528	0.968502	0.353196	0.061*
C13A	0.7670 (2)	0.89859 (15)	0.48275 (13)	0.0564 (4)
H13A	0.807925	0.974694	0.538940	0.068*
C14A	0.72841 (16)	0.79222 (15)	0.51154 (13)	0.0516 (4)
H14A	0.742334	0.794838	0.587398	0.062*
C15A	0.66983 (16)	0.68256 (15)	0.43028 (14)	0.0528 (4)
H15A	0.643701	0.609288	0.450356	0.063*
C16A	0.64825 (14)	0.67748 (12)	0.31873 (13)	0.0443 (3)
H16A	0.607769	0.601082	0.263057	0.053*
O1B	0.67935 (10)	0.46416 (8)	0.56167 (8)	0.0430 (2)
O2B	0.58550 (10)	0.10049 (8)	0.64236 (8)	0.0450 (2)
N1B	0.65081 (11)	0.29799 (9)	0.63038 (9)	0.0367 (2)
N2B	0.58273 (12)	0.14933 (9)	0.47865 (9)	0.0370 (2)

C1B	0.60271 (12)	0.17176 (11)	0.58711 (10)	0.0357 (3)
C2B	0.65096 (13)	0.35657 (10)	0.54846 (10)	0.0342 (3)
C3B	0.61432 (13)	0.25927 (10)	0.44140 (10)	0.0335 (3)
C4B	0.69356 (16)	0.35873 (13)	0.74856 (11)	0.0461 (3)
H4BA	0.641547	0.411788	0.748697	0.055*
H4BB	0.669560	0.297129	0.787415	0.055*
C41B	0.84330 (18)	0.43143 (14)	0.81171 (12)	0.0557 (4)
C42B	0.9646 (2)	0.4894 (2)	0.86070 (17)	0.0882 (7)
H42B	1.062699	0.536214	0.900302	0.106*
C5B	0.48929 (12)	0.24919 (10)	0.33036 (10)	0.0330 (3)
C6B	0.41792 (14)	0.32636 (11)	0.32142 (11)	0.0393 (3)
H6B	0.446357	0.390018	0.386763	0.047*
C7B	0.30456 (15)	0.31056 (13)	0.21666 (13)	0.0473 (3)
H7B	0.255485	0.363157	0.211075	0.057*
C8B	0.26317 (15)	0.21903 (14)	0.12106 (12)	0.0488 (3)
H8B	0.186476	0.209149	0.049625	0.059*
C9B	0.33373 (16)	0.14167 (13)	0.12955 (12)	0.0477 (3)
H9B	0.305049	0.078260	0.063919	0.057*
C10B	0.44609 (14)	0.15641 (12)	0.23347 (11)	0.0405 (3)
H10B	0.494054	0.102919	0.238765	0.049*
C11B	0.74665 (13)	0.28834 (11)	0.42686 (10)	0.0369 (3)
C12B	0.77757 (15)	0.37651 (13)	0.37318 (12)	0.0454 (3)
H12B	0.716546	0.417811	0.345115	0.054*
C13B	0.89756 (17)	0.40443 (15)	0.36044 (14)	0.0567 (4)
H13B	0.918590	0.465199	0.324107	0.068*
C14B	0.98625 (18)	0.34451 (17)	0.40019 (17)	0.0660 (5)
H14B	1.066874	0.362105	0.389500	0.079*
C15B	0.9570 (2)	0.25872 (19)	0.4557 (2)	0.0767 (6)
H15B	1.018882	0.218367	0.484605	0.092*
C16B	0.83838 (17)	0.23106 (15)	0.46947 (17)	0.0584 (4)
H16B	0.819719	0.172392	0.508422	0.070*
H2A	0.613 (2)	0.5994 (18)	0.0919 (16)	0.062 (5)*
H2B	0.5382 (19)	0.0745 (17)	0.4319 (15)	0.052 (4)*

Atomic displacement parameters (Å²)

	U^{11}	U^{22}	U^{33}	U^{12}	U^{13}	U^{23}
O1A	0.0576 (6)	0.0257 (4)	0.0468 (5)	0.0196 (4)	0.0199 (4)	0.0109 (4)
O2A	0.0652 (7)	0.0305 (5)	0.0486 (6)	0.0210 (5)	−0.0007 (5)	0.0020 (4)
N1A	0.0456 (6)	0.0270 (5)	0.0393 (5)	0.0178 (4)	0.0128 (5)	0.0107 (4)
N2A	0.0508 (6)	0.0253 (5)	0.0426 (6)	0.0194 (5)	0.0092 (5)	0.0058 (4)
C1A	0.0514 (7)	0.0281 (6)	0.0403 (7)	0.0183 (5)	0.0128 (6)	0.0088 (5)
C2A	0.0445 (7)	0.0270 (6)	0.0387 (6)	0.0158 (5)	0.0193 (5)	0.0125 (5)
C3A	0.0430 (6)	0.0248 (5)	0.0367 (6)	0.0148 (5)	0.0146 (5)	0.0089 (4)
C4A	0.0497 (7)	0.0347 (6)	0.0410 (7)	0.0221 (6)	0.0147 (6)	0.0155 (5)
C41A	0.0560 (8)	0.0432 (7)	0.0516 (8)	0.0255 (7)	0.0188 (7)	0.0121 (6)
C42A	0.0821 (14)	0.0934 (15)	0.0926 (15)	0.0474 (12)	0.0511 (12)	0.0238 (12)
C5A	0.0444 (7)	0.0429 (7)	0.0286 (6)	0.0176 (5)	0.0155 (5)	0.0101 (5)

C6A	0.0473 (7)	0.0449 (7)	0.0413 (7)	0.0109 (6)	0.0165 (6)	0.0115 (6)
C7A	0.0527 (9)	0.0662 (10)	0.0514 (9)	0.0051 (8)	0.0209 (7)	0.0149 (7)
C8A	0.0474 (9)	0.0962 (14)	0.0509 (9)	0.0189 (9)	0.0241 (7)	0.0170 (9)
C9A	0.0580 (10)	0.0944 (14)	0.0610 (10)	0.0422 (10)	0.0305 (8)	0.0248 (9)
C10A	0.0572 (9)	0.0604 (9)	0.0570 (9)	0.0320 (7)	0.0294 (7)	0.0228 (7)
C11A	0.0398 (6)	0.0322 (6)	0.0412 (6)	0.0167 (5)	0.0188 (5)	0.0158 (5)
C12A	0.0766 (10)	0.0347 (7)	0.0447 (7)	0.0206 (7)	0.0322 (7)	0.0162 (6)
C13A	0.0808 (11)	0.0509 (8)	0.0451 (8)	0.0290 (8)	0.0331 (8)	0.0176 (6)
C14A	0.0557 (8)	0.0652 (9)	0.0489 (8)	0.0288 (7)	0.0307 (7)	0.0302 (7)
C15A	0.0506 (8)	0.0533 (8)	0.0632 (9)	0.0196 (7)	0.0296 (7)	0.0367 (7)
C16A	0.0434 (7)	0.0346 (6)	0.0525 (8)	0.0132 (5)	0.0200 (6)	0.0199 (6)
O1B	0.0573 (6)	0.0272 (4)	0.0411 (5)	0.0150 (4)	0.0212 (4)	0.0092 (3)
O2B	0.0517 (5)	0.0347 (5)	0.0369 (5)	0.0087 (4)	0.0145 (4)	0.0155 (4)
N1B	0.0423 (5)	0.0299 (5)	0.0317 (5)	0.0109 (4)	0.0142 (4)	0.0084 (4)
N2B	0.0461 (6)	0.0243 (5)	0.0351 (5)	0.0105 (4)	0.0164 (4)	0.0094 (4)
C1B	0.0343 (6)	0.0295 (6)	0.0350 (6)	0.0089 (5)	0.0111 (5)	0.0102 (5)
C2B	0.0365 (6)	0.0286 (6)	0.0335 (6)	0.0114 (5)	0.0139 (5)	0.0083 (4)
C3B	0.0401 (6)	0.0242 (5)	0.0344 (6)	0.0111 (5)	0.0167 (5)	0.0093 (4)
C4B	0.0565 (8)	0.0412 (7)	0.0344 (6)	0.0142 (6)	0.0202 (6)	0.0079 (5)
C41B	0.0659 (10)	0.0440 (8)	0.0355 (7)	0.0108 (7)	0.0134 (7)	0.0062 (6)
C42B	0.0675 (12)	0.0817 (14)	0.0557 (11)	−0.0076 (11)	0.0054 (9)	0.0042 (9)
C5B	0.0357 (6)	0.0294 (5)	0.0341 (6)	0.0096 (5)	0.0181 (5)	0.0115 (4)
C6B	0.0458 (7)	0.0348 (6)	0.0397 (6)	0.0167 (5)	0.0212 (5)	0.0126 (5)
C7B	0.0504 (8)	0.0481 (8)	0.0487 (8)	0.0255 (6)	0.0217 (6)	0.0212 (6)
C8B	0.0439 (7)	0.0570 (8)	0.0387 (7)	0.0173 (6)	0.0139 (6)	0.0176 (6)
C9B	0.0509 (8)	0.0478 (7)	0.0351 (7)	0.0141 (6)	0.0172 (6)	0.0053 (5)
C10B	0.0432 (7)	0.0381 (6)	0.0384 (6)	0.0157 (5)	0.0186 (5)	0.0082 (5)
C11B	0.0373 (6)	0.0303 (6)	0.0353 (6)	0.0093 (5)	0.0145 (5)	0.0038 (5)
C12B	0.0433 (7)	0.0454 (7)	0.0433 (7)	0.0119 (6)	0.0200 (6)	0.0142 (6)
C13B	0.0489 (8)	0.0583 (9)	0.0491 (8)	0.0026 (7)	0.0253 (7)	0.0089 (7)
C14B	0.0443 (8)	0.0671 (10)	0.0767 (11)	0.0096 (8)	0.0330 (8)	0.0020 (9)
C15B	0.0524 (10)	0.0679 (11)	0.1175 (17)	0.0294 (9)	0.0429 (11)	0.0260 (11)
C16B	0.0499 (8)	0.0485 (8)	0.0838 (11)	0.0233 (7)	0.0332 (8)	0.0257 (8)

Geometric parameters (Å, º)

O1A—C2A	1.2098 (15)	O1B—C2B	1.2062 (15)
O2A—C1A	1.2240 (16)	O2B—C1B	1.2192 (15)
N1A—C2A	1.3638 (16)	N1B—C2B	1.3690 (16)
N1A—C1A	1.3962 (15)	N1B—C1B	1.4006 (15)
N1A—C4A	1.4581 (16)	N1B—C4B	1.4550 (16)
N2A—C1A	1.3394 (18)	N2B—C1B	1.3434 (16)
N2A—C3A	1.4624 (15)	N2B—C3B	1.4647 (14)
N2A—H2A	0.88 (2)	N2B—H2B	0.885 (18)
C2A—C3A	1.5438 (16)	C2B—C3B	1.5427 (16)
C3A—C11A	1.5311 (18)	C3B—C5B	1.5276 (16)
C3A—C5A	1.5332 (19)	C3B—C11B	1.5365 (17)
C4A—C41A	1.456 (2)	C4B—C41B	1.454 (2)

C4A—H4AA	0.9900	C4B—H4BA	0.9900
C4A—H4AB	0.9900	C4B—H4BB	0.9900
C41A—C42A	1.171 (3)	C41B—C42B	1.175 (3)
C42A—H42A	0.9500	C42B—H42B	0.9500
C5A—C6A	1.385 (2)	C5B—C6B	1.3877 (18)
C5A—C10A	1.390 (2)	C5B—C10B	1.3941 (17)
C6A—C7A	1.390 (2)	C6B—C7B	1.3936 (19)
C6A—H6A	0.9500	C6B—H6B	0.9500
C7A—C8A	1.371 (3)	C7B—C8B	1.379 (2)
C7A—H7A	0.9500	C7B—H7B	0.9500
C8A—C9A	1.370 (3)	C8B—C9B	1.383 (2)
C8A—H8A	0.9500	C8B—H8B	0.9500
C9A—C10A	1.387 (2)	C9B—C10B	1.3851 (19)
C9A—H9A	0.9500	C9B—H9B	0.9500
C10A—H10A	0.9500	C10B—H10B	0.9500
C11A—C16A	1.3861 (17)	C11B—C16B	1.384 (2)
C11A—C12A	1.3896 (19)	C11B—C12B	1.3886 (18)
C12A—C13A	1.381 (2)	C12B—C13B	1.389 (2)
C12A—H12A	0.9500	C12B—H12B	0.9500
C13A—C14A	1.378 (2)	C13B—C14B	1.378 (3)
C13A—H13A	0.9500	C13B—H13B	0.9500
C14A—C15A	1.371 (2)	C14B—C15B	1.380 (3)
C14A—H14A	0.9500	C14B—H14B	0.9500
C15A—C16A	1.391 (2)	C15B—C16B	1.382 (2)
C15A—H15A	0.9500	C15B—H15B	0.9500
C16A—H16A	0.9500	C16B—H16B	0.9500

C2A—N1A—C1A	112.05 (10)	C2B—N1B—C1B	112.22 (10)
C2A—N1A—C4A	124.18 (10)	C2B—N1B—C4B	124.32 (10)
C1A—N1A—C4A	123.76 (11)	C1B—N1B—C4B	123.46 (10)
C1A—N2A—C3A	113.62 (10)	C1B—N2B—C3B	113.42 (10)
C1A—N2A—H2A	120.4 (13)	C1B—N2B—H2B	121.1 (11)
C3A—N2A—H2A	126.0 (13)	C3B—N2B—H2B	124.3 (11)
O2A—C1A—N2A	128.83 (12)	O2B—C1B—N2B	129.21 (11)
O2A—C1A—N1A	123.93 (12)	O2B—C1B—N1B	123.82 (12)
N2A—C1A—N1A	107.24 (11)	N2B—C1B—N1B	106.96 (10)
O1A—C2A—N1A	125.27 (11)	O1B—C2B—N1B	125.31 (11)
O1A—C2A—C3A	127.78 (11)	O1B—C2B—C3B	128.21 (11)
N1A—C2A—C3A	106.95 (9)	N1B—C2B—C3B	106.44 (9)
N2A—C3A—C11A	113.17 (10)	N2B—C3B—C5B	110.86 (9)
N2A—C3A—C5A	111.85 (11)	N2B—C3B—C11B	112.38 (10)
C11A—C3A—C5A	108.63 (10)	C5B—C3B—C11B	110.51 (9)
N2A—C3A—C2A	100.12 (9)	N2B—C3B—C2B	100.51 (9)
C11A—C3A—C2A	110.22 (10)	C5B—C3B—C2B	115.22 (10)
C5A—C3A—C2A	112.73 (10)	C11B—C3B—C2B	107.02 (9)
C41A—C4A—N1A	112.40 (11)	C41B—C4B—N1B	111.36 (13)
C41A—C4A—H4AA	109.1	C41B—C4B—H4BA	109.4
N1A—C4A—H4AA	109.1	N1B—C4B—H4BA	109.4

C41A—C4A—H4AB	109.1	C41B—C4B—H4BB	109.4
N1A—C4A—H4AB	109.1	N1B—C4B—H4BB	109.4
H4AA—C4A—H4AB	107.9	H4BA—C4B—H4BB	108.0
C42A—C41A—C4A	179.38 (19)	C42B—C41B—C4B	178.6 (2)
C41A—C42A—H42A	180.0	C41B—C42B—H42B	180.0
C6A—C5A—C10A	118.73 (14)	C6B—C5B—C10B	119.12 (11)
C6A—C5A—C3A	122.97 (12)	C6B—C5B—C3B	123.80 (11)
C10A—C5A—C3A	118.21 (12)	C10B—C5B—C3B	117.08 (11)
C5A—C6A—C7A	120.32 (15)	C5B—C6B—C7B	120.06 (12)
C5A—C6A—H6A	119.8	C5B—C6B—H6B	120.0
C7A—C6A—H6A	119.8	C7B—C6B—H6B	120.0
C8A—C7A—C6A	120.52 (17)	C8B—C7B—C6B	120.41 (13)
C8A—C7A—H7A	119.7	C8B—C7B—H7B	119.8
C6A—C7A—H7A	119.7	C6B—C7B—H7B	119.8
C9A—C8A—C7A	119.53 (16)	C7B—C8B—C9B	119.77 (13)
C9A—C8A—H8A	120.2	C7B—C8B—H8B	120.1
C7A—C8A—H8A	120.2	C9B—C8B—H8B	120.1
C8A—C9A—C10A	120.74 (17)	C8B—C9B—C10B	120.18 (13)
C8A—C9A—H9A	119.6	C8B—C9B—H9B	119.9
C10A—C9A—H9A	119.6	C10B—C9B—H9B	119.9
C9A—C10A—C5A	120.14 (16)	C9B—C10B—C5B	120.45 (12)
C9A—C10A—H10A	119.9	C9B—C10B—H10B	119.8
C5A—C10A—H10A	119.9	C5B—C10B—H10B	119.8
C16A—C11A—C12A	119.00 (12)	C16B—C11B—C12B	119.12 (13)
C16A—C11A—C3A	121.92 (12)	C16B—C11B—C3B	121.29 (12)
C12A—C11A—C3A	118.98 (11)	C12B—C11B—C3B	119.56 (11)
C13A—C12A—C11A	120.61 (13)	C11B—C12B—C13B	120.12 (14)
C13A—C12A—H12A	119.7	C11B—C12B—H12B	119.9
C11A—C12A—H12A	119.7	C13B—C12B—H12B	119.9
C14A—C13A—C12A	120.14 (15)	C14B—C13B—C12B	120.38 (15)
C14A—C13A—H13A	119.9	C14B—C13B—H13B	119.8
C12A—C13A—H13A	119.9	C12B—C13B—H13B	119.8
C15A—C14A—C13A	119.74 (14)	C13B—C14B—C15B	119.45 (15)
C15A—C14A—H14A	120.1	C13B—C14B—H14B	120.3
C13A—C14A—H14A	120.1	C15B—C14B—H14B	120.3
C14A—C15A—C16A	120.70 (13)	C14B—C15B—C16B	120.52 (17)
C14A—C15A—H15A	119.7	C14B—C15B—H15B	119.7
C16A—C15A—H15A	119.7	C16B—C15B—H15B	119.7
C11A—C16A—C15A	119.80 (13)	C15B—C16B—C11B	120.37 (16)
C11A—C16A—H16A	120.1	C15B—C16B—H16B	119.8
C15A—C16A—H16A	120.1	C11B—C16B—H16B	119.8

C3A—N2A—C1A—O2A	−178.94 (16)	C3B—N2B—C1B—O2B	179.76 (13)
C3A—N2A—C1A—N1A	0.59 (17)	C3B—N2B—C1B—N1B	−0.82 (14)
C2A—N1A—C1A—O2A	178.13 (15)	C2B—N1B—C1B—O2B	−175.41 (12)
C4A—N1A—C1A—O2A	−2.1 (2)	C4B—N1B—C1B—O2B	3.8 (2)
C2A—N1A—C1A—N2A	−1.43 (17)	C2B—N1B—C1B—N2B	5.13 (14)
C4A—N1A—C1A—N2A	178.33 (12)	C4B—N1B—C1B—N2B	−175.67 (12)

C1A—N1A—C2A—O1A	−178.06 (13)	C1B—N1B—C2B—O1B	175.24 (12)
C4A—N1A—C2A—O1A	2.2 (2)	C4B—N1B—C2B—O1B	−3.9 (2)
C1A—N1A—C2A—C3A	1.63 (15)	C1B—N1B—C2B—C3B	−7.01 (14)
C4A—N1A—C2A—C3A	−178.13 (12)	C4B—N1B—C2B—C3B	173.80 (12)
C1A—N2A—C3A—C11A	117.61 (13)	C1B—N2B—C3B—C5B	−125.40 (11)
C1A—N2A—C3A—C5A	−119.29 (13)	C1B—N2B—C3B—C11B	110.38 (12)
C1A—N2A—C3A—C2A	0.34 (15)	C1B—N2B—C3B—C2B	−3.09 (13)
O1A—C2A—C3A—N2A	178.52 (13)	O1B—C2B—C3B—N2B	−176.45 (13)
N1A—C2A—C3A—N2A	−1.16 (13)	N1B—C2B—C3B—N2B	5.88 (12)
O1A—C2A—C3A—C11A	59.07 (17)	O1B—C2B—C3B—C5B	−57.26 (17)
N1A—C2A—C3A—C11A	−120.61 (11)	N1B—C2B—C3B—C5B	125.07 (11)
O1A—C2A—C3A—C5A	−62.49 (17)	O1B—C2B—C3B—C11B	66.05 (16)
N1A—C2A—C3A—C5A	117.83 (11)	N1B—C2B—C3B—C11B	−111.62 (11)
C2A—N1A—C4A—C41A	−80.14 (16)	C2B—N1B—C4B—C41B	−68.42 (17)
C1A—N1A—C4A—C41A	100.12 (16)	C1B—N1B—C4B—C41B	112.48 (14)
N2A—C3A—C5A—C6A	132.60 (12)	N2B—C3B—C5B—C6B	117.89 (12)
C11A—C3A—C5A—C6A	−101.77 (13)	C11B—C3B—C5B—C6B	−116.84 (12)
C2A—C3A—C5A—C6A	20.69 (16)	C2B—C3B—C5B—C6B	4.61 (16)
N2A—C3A—C5A—C10A	−50.88 (15)	N2B—C3B—C5B—C10B	−62.07 (14)
C11A—C3A—C5A—C10A	74.75 (14)	C11B—C3B—C5B—C10B	63.20 (13)
C2A—C3A—C5A—C10A	−162.79 (12)	C2B—C3B—C5B—C10B	−175.35 (10)
C10A—C5A—C6A—C7A	1.4 (2)	C10B—C5B—C6B—C7B	0.08 (19)
C3A—C5A—C6A—C7A	177.91 (13)	C3B—C5B—C6B—C7B	−179.87 (12)
C5A—C6A—C7A—C8A	−1.7 (2)	C5B—C6B—C7B—C8B	−0.5 (2)
C6A—C7A—C8A—C9A	1.0 (3)	C6B—C7B—C8B—C9B	0.7 (2)
C7A—C8A—C9A—C10A	0.0 (3)	C7B—C8B—C9B—C10B	−0.4 (2)
C8A—C9A—C10A—C5A	−0.3 (3)	C8B—C9B—C10B—C5B	−0.1 (2)
C6A—C5A—C10A—C9A	−0.4 (2)	C6B—C5B—C10B—C9B	0.22 (19)
C3A—C5A—C10A—C9A	−177.07 (14)	C3B—C5B—C10B—C9B	−179.82 (12)
N2A—C3A—C11A—C16A	10.63 (17)	N2B—C3B—C11B—C16B	−13.23 (17)
C5A—C3A—C11A—C16A	−114.22 (13)	C5B—C3B—C11B—C16B	−137.64 (13)
C2A—C3A—C11A—C16A	121.81 (13)	C2B—C3B—C11B—C16B	96.18 (14)
N2A—C3A—C11A—C12A	−172.91 (12)	N2B—C3B—C11B—C12B	168.84 (11)
C5A—C3A—C11A—C12A	62.23 (15)	C5B—C3B—C11B—C12B	44.43 (15)
C2A—C3A—C11A—C12A	−61.73 (16)	C2B—C3B—C11B—C12B	−81.75 (13)
C16A—C11A—C12A—C13A	−0.7 (2)	C16B—C11B—C12B—C13B	1.4 (2)
C3A—C11A—C12A—C13A	−177.27 (14)	C3B—C11B—C12B—C13B	179.41 (12)
C11A—C12A—C13A—C14A	0.3 (3)	C11B—C12B—C13B—C14B	0.4 (2)
C12A—C13A—C14A—C15A	0.2 (3)	C12B—C13B—C14B—C15B	−1.8 (3)
C13A—C14A—C15A—C16A	−0.3 (2)	C13B—C14B—C15B—C16B	1.3 (3)
C12A—C11A—C16A—C15A	0.6 (2)	C14B—C15B—C16B—C11B	0.6 (3)
C3A—C11A—C16A—C15A	177.08 (12)	C12B—C11B—C16B—C15B	−1.9 (2)
C14A—C15A—C16A—C11A	−0.1 (2)	C3B—C11B—C16B—C15B	−179.86 (16)

Hydrogen-bond geometry (Å, º)

*Cg*2 and *Cg*3 are the centroids of the C5*A*–C10*A* and C11*A*–C16*A* benzene rings, respectively.

D—H···*A*	*D*—H	H···*A*	*D*···*A*	*D*—H···*A*
N2*A*—H2*A*···O2*A*^{i}	0.88 (2)	1.99 (2)	2.855 (2)	167 (2)
N2*B*—H2*BB*···O2*B*^{ii}	0.89 (2)	1.99 (2)	2.847 (1)	163 (2)
C4*A*—H4*AA*···O1*A*^{iii}	0.99	2.31	3.253 (2)	160
C15*A*—H15*A*···O1*B*	0.95	2.44	3.332 (2)	156
C8*B*—H8*B*···*Cg*2^{i}	0.95	2.88	3.713 (2)	147
C15*B*—H15*B*···*Cg*3^{iv}	0.95	2.87	3.742 (3)	153

Symmetry codes: (i) −*x*+1, −*y*+1, −*z*; (ii) −*x*+1, −*y*, −*z*+1; (iii) −*x*+1, −*y*+2, −*z*; (iv) −*x*+2, −*y*+1, −*z*+1.